Submitted to *J. Phys.: Condens. Matter*

Date: 22 September 2012

The bound coherent neutron scattering lengths of the oxygen isotopes

Henry E. Fischer[a], J. Mike Simonson[b], Jörg C. Neuefeind[c], Hartmut Lemmel[a,d], Helmut Rauch[a,d], Anita Zeidler[e] and Philip S. Salmon[e]

[a] Institut Laue-Langevin, 6 rue Jules Horowitz, B.P. 156, 38042 Grenoble cedex 9, France

[b] Center for Nanophase Materials Sciences, Oak Ridge National Laboratory, P.O. Box 2008 MS 6493, Oak Ridge, TN 37831, USA

[c] Spallation Neutron Source, Oak Ridge National Laboratory, P.O. Box 2008 MS 6474, Oak Ridge, TN 37831, USA

[d] Vienna University of Technology, Atominstitut, Stadionallee 2, 1020 Wien, Österreich

[e] Department of Physics, University of Bath, Bath BA2 7AY, United Kingdom

E-mail: `fischer@ill.fr`

Abstract. The technique of neutron interferometry was used to measure the bound coherent neutron scattering length $b_{\rm coh}$ of the oxygen isotopes ^{17}O and ^{18}O. From the measured difference in optical path between two water samples, either $H_2{}^{17}O$ or $H_2{}^{18}O$ versus $H_2{}^{\rm nat}O$, where nat denotes the natural isotopic composition, we obtain $b_{\rm coh,17O} = 5.867(4)$ fm and $b_{\rm coh,18O} = 6.009(5)$ fm, based on the accurately known value of $b_{\rm coh,natO} = 5.805(4)$ fm which is equal to $b_{\rm coh,16O}$ within the experimental uncertainty. Our results for $b_{\rm coh,17O}$ and $b_{\rm coh,18O}$ differ appreciably from the standard tabulated values of 5.6(5) fm and 5.84(7) fm, respectively. In particular, our measured scattering-length contrast of 0.204(3) fm between ^{18}O and $^{\rm nat}$O is nearly a factor of 6 greater than the tabulated value, which renders feasible neutron diffraction experiments using ^{18}O isotope substitution and thereby offers new possibilites for measuring the partial structure factors of oxygen-containing compounds, such as water.

PACS numbers: 61.12.-q: Neutron diffraction and scattering, 03.75.Dg: Atom and neutron interferometry

Keywords: neutron scattering lengths, neutron interferometry, neutron diffraction, oxygen isotopes, isotope substitution

1. Introduction

Of fundamental utility to all neutron scattering techniques, the values of neutron scattering lengths for stable isotopes should be measured by experiment, even in cases where theoretical predictions can be made. The bound coherent b_{coh} and incoherent b_{incoh} neutron scattering lengths listed in today's standard tables (*e.g.* Rauch and Waschkowski 2003, Aleksejevs *et al* 1998, Sears 1992, Koester *et al* 1991, Mughabghab *et al* 1981) date largely from measurements performed decades ago and often have large experimental uncertainties or even recognizable systematic errors. These uncertainties are becoming a significant limitation to the attainable accuracy of neutron diffraction data, given the improvements offered by modern neutron diffraction instrumentation in terms of low systematic error and high counting statistics precision (*e.g.* Fischer *et al* 2002, Zeidler *et al* 2012).

In particular, the technique of neutron diffraction with isotope substitution (NDIS) (*e.g.* Fischer *et al* 2006, sec 3.2), wherein chemically identical samples are prepared having different isotopic compositions, allows for a complete element-specific determination of the structure of materials in terms of partial structure factors (PSFs), but relies on accurate knowledge of the bound coherent scattering lengths b_{coh} for the isotopes of a given element. In the case when the scattering-length contrast Δb_{coh} between two isotopes is rather small ($\lesssim 0.5$ fm), inaccuracies in the b_{coh} values can lead to large relative errors.

We therefore decided to launch a program to measure the bound coherent neutron scattering lengths of various isotopes using the sensitive technique of neutron interferometry (*e.g.* Rauch and Werner 2000). Our first interferometry experiment measured b_{coh} for the ^{13}C isotope to high accuracy (Fischer *et al* 2008), giving a value that differed significantly from a previous standard value measured by Koester *et al* (1979). Our result not only explained a long-standing problem in NDIS experiments employing carbon isotope substitution, but provided an accurate scattering length value for ^{13}C that was used for a PSF analysis of the structures of liquid CS_2 and liquid CO_2 (Neuefeind *et al* 2009).

The element oxygen plays a major role in the structure and properties of many materials, including water. For the latter, more accurate values of scattering lengths for the O isotopes could allow a PSF determination using neutron diffraction without recourse to H/D isotope substitution (*e.g.* Soper 1997, Neilson and Adya 1996), which is prone to quantum effects (Egelstaff 2002, 2003) and uncertainties in corrections for inelastic scattering (*e.g.* Salmon *et al* 2004).

The most recent compilation of bound coherent neutron scattering lengths (Rauch and Waschkowski 2003) lists recommended values of 5.805(4) fm for $^{\mathrm{nat}}$O, where "nat" denotes the natural isotopic composition, 5.805(5) fm for ^{16}O, 5.6(5) fm for ^{17}O and 5.84(7) fm for ^{18}O. The isotopes ^{17}O and ^{18}O have natural abundances of 0.039 % and 0.208 %, respectively, the remainder being made up by ^{16}O. These recommended b_{coh} values for oxygen are due to Koester *et al* (1979) and are based on an analysis

of Christiansen filter measurements and gravity refractometry results. As compounds containing ^{nat}O are generally available in large quantities of high chemical purity, b_{coh} can be measured accurately with less difficulty for ^{nat}O as compared to ^{17}O or ^{18}O, and in fact Koester *et al* (1991) lists very reproducible values for $b_{coh,natO}$ as obtained by different experimental teams.

By contrast, the experimental results for $b_{coh,17O}$ and $b_{coh,18O}$ are fewer in number, have larger reported uncertainties, and are considerably less reproducible than is the case for $b_{coh,natO}$. For example, Koester *et al* (1991) lists the 5.78(15) fm result for $b_{coh,17O}$ by Valentine (1968) using Bragg diffraction from a ^{17}O-enriched UO_2 single crystal, and the 6.01(13) fm result for $b_{coh,18O}$ by O'Connor (1967) using Bragg diffraction from ^{18}O-enriched $UO_{2.010}$ single crystals. These b_{coh} values from Bragg diffraction differ appreciably from the recommended values tabulated by Rauch and Waschkowski (2003).

In view of the sparcity, considerable experimental uncertainties, and relatively poor mutual agreement in the literature values for b_{coh} of the oxygen isotopes ^{17}O and ^{18}O, and considering the importance of accurate values for these bound coherent neutron scattering lengths vis-à-vis NDIS studies, we undertook neutron interferometry experiments to measure $b_{coh,17O}$ and $b_{coh,18O}$. Since our first interferometry study (Fischer *et al* 2008), we have improved and better characterised the experimental technique for measuring accurately the difference in average scattering length between two liquid samples. In this case, the samples were light water enriched in either ^{17}O or ^{18}O isotopes as compared to $H_2{}^{nat}O$.

2. Description of the neutron interferometry experiments

2.1. Measurement of the average bound coherent scattering length $\overline{b}$

Neutron interferometry (*e.g.* Rauch and Werner 2000) is analogous to photon interferometry and provides a very accurate method for measuring bound coherent scattering lengths. For most materials, the index of refraction n for thermal neutrons (kinetic energy $E \sim 25$ meV, wavelength $\lambda \sim 1.8$ Å) is slightly less than unity and well-approximated by

$$n \;=\; 1 \,-\, \lambda^2 \, N \, \overline{b} \,/\, 2\pi \;, \tag{2.1}$$

where $\overline{b}$ (usually > 0) is the bound coherent neutron scattering length averaged over all the atoms in the material, and N is the number density of atoms. Note that the product $N\overline{b}$ represents the material's scattering-length density. A rectangular slab of such material of thickness D has an optical path length of $L = nD < D$, and thus the presence of the slab induces an optical path difference of $\Delta L = (n-1)D$ as compared to vacuum. A neutron of wavevector $k = 2\pi/\lambda$ traversing the slab perpendicularly will thereby acquire a wavefunction phase shift (in radians) of

$$\phi \;=\; k \, \Delta L \;=\; k \, (n-1) \, D \;=\; -\, \lambda \, N \, \overline{b} \, D \tag{2.2}$$

relative to a trajectory of length D in vacuum. In general practice, ϕ can be measured interferometrically to a precision of $\lesssim 1^\circ$. By splitting a neutron's wavefunction into two

parts, one traversing the slab and the other not, and then recombining the two parts coherently via interference, one can measure a difference in optical path ΔL induced by the slab that is considerably smaller than one neutron wavelength, which leads to a very accurate determination of $\overline{b}$ in the material, provided that λ, N and D are accurately known.

Note that neutron interferometry is based on quantum self-interference of neutrons. Each individual neutron's wavefunction is a coherent superposition of states propagating simultaneously along two different paths of the interferometer that are separated by macroscopic distances (several cm) much larger than typical neutron coherence lengths of order 100 Å. Various neutron interferometer geometries can be used, having advantages and disadvantages for different types of neutron interference measurements (see Lemmel and Wagh (2010) for a critical discussion).

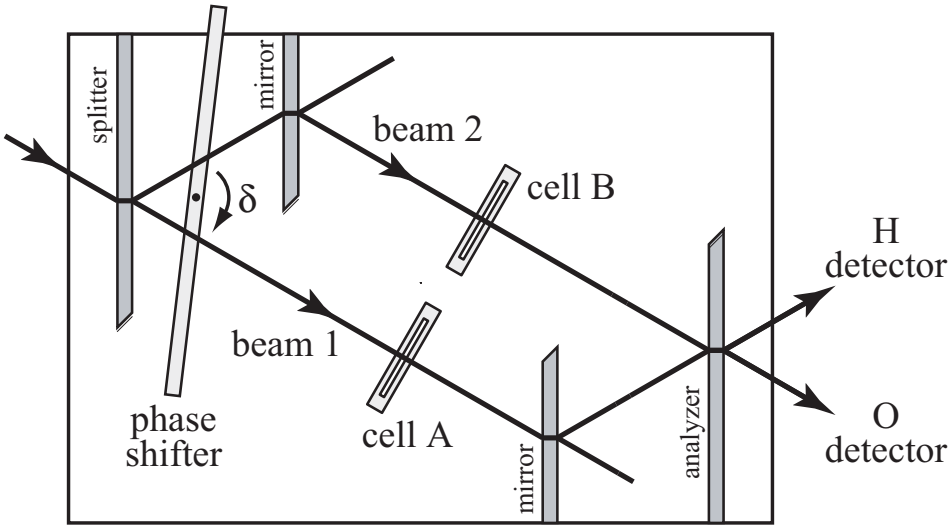

Figure 1. Top view schematic of the single-crystal Si neutron interferometer of skew-symmetric geometry that was used for the bound coherent neutron scattering-length measurements. The longitudinal dimension of the interferometer is about 15 cm, and the thickness of the four protruding Si "blades" is about 3 mm. The phase-shifter slab, here placed upstream of the samples, is also made of monocrystalline Si with thickness $\sim$ 5 mm. The samples held in Hellma cells can be lowered into place from above, and neither the samples nor the phase-shifter ever make physical contact with the interferometer crystal. The incident neutron's wavefunction is divided by the splitter blade into a transmitted ("beam 1") and a diffracted ("beam 2") component. The two mirror blades serve to redirect the two beams along parallel paths, separated by about 32 mm. Different samples placed in the two beams modify differently the optical path lengths of the two wavefunction components, which thereby accumulate a relative phase difference $\Delta\phi$ that affects their interference when recombined at the analyser blade, and thereby the probability that the neutron will be detected along a parallel trajectory by the "O" detector, or along a diffracted trajectory by the "H" detector. The phase-shifter is scanned in angle δ about a vertical axis, thus inducing a variable additional phase shift between the two paths of the split wavefunction. The counting rate of either the O or H detector, measured as a function of the phase-shifter angle with and without the samples in position, allows $\Delta\phi$ to be determined.

2.2. Differential mode for measuring $\Delta\overline{b}$

The neutron interferometry experiments were performed using the S18 instrument (*e.g.* Kroupa *et al* 2000) at the Institut Laue-Langevin (ILL) in Grenoble, France, and employed a single-crystal Si neutron interferometer of skew-symmetric geometry, which is illustrated schematically in figure 1. An incident neutron's wavefunction is split into beams "1" and "2" that pass separately through two samples before being recombined downstream. An advantage of the skew-symmetric geometry is that it allows both samples to be placed perpendicular to their respective beams, which facilitates the calculation via equation (2.2) of the phase shifts ϕ_1 and ϕ_2 induced by the samples in beams 1 and 2, respectively. The choice of sign convention

$$\Delta\phi = \phi_1 - \phi_2 \tag{2.3}$$

then leads to $\Delta\phi > 0$ when beam 1 has a greater optical path than beam 2. This $\Delta\phi$ can be revealed and precisely measured by performing a "phase-shifter scan", wherein the counting rate of either of the two detectors (traditionally named "O" for a parallel exit and "H" for a diffracted exit from the interferometer) is measured as a function of the additional phase shift induced by a small change in the angle δ of a phase-shifter slab placed upstream† of the samples (Rauch and Werner 2000, Eqn. 2.7). Note that the O and H detector counts are always exactly 180° out of phase in ϕ with respect to each other, due to conservation of probability (*i.e.* a given neutron is captured by only one or the other detector).

Since the neutron wavelength λ for both beams is necessarily identical, one can place a sample of known scattering-length density in one beam, and a sample of unknown scattering-length density in the other beam, thus offering a more sensitive and precise *differential mode* of scattering-length measurement. If the two samples also have the same thickness D and the same atomic number density N (as can be the case for isotopically enriched samples), then the equation for the measured phase difference (in radians) becomes:

$$\Delta\phi \;=\; \lambda\, N\, \Delta\overline{b}\, D\;, \tag{2.4}$$

where $\Delta\overline{b}$ is the difference in bound coherent scattering length between the two samples as averaged over all atoms in each sample. Equation (2.3) then implies $\Delta\phi > 0$ when the sample in beam 2 has the greater (*i.e.* more positive) average scattering length $\overline{b}$.

Note however that the phase difference measured for the empty interferometer is not zero, due to imperfections in the interferometer geometry and an arbitrary angle

† In the earlier interferometry experiment (Fischer *et al* 2008), the same interferometer at the S18 instrument was used, except that the phase-shifter was mounted downstream of the samples, so that its effect on the relative optical path lengths for beams 1 versus 2 was reversed for a given rotation angle. As we chose to retain the same definition of $\delta > 0$ for clockwise rotation as viewed from above, so that the relation between $\Delta\phi$ and δ remained the same, our expression for $\Delta\phi$ changed from $\phi_2 - \phi_1$ in the previous experiment to $\phi_1 - \phi_2$ for the present experiments. The latter expression leads to $\Delta\phi > 0$ when the sample in beam 2 has the greater scattering-length density for our differential-mode measurements, a convention that is chosen since the sample in beam 1 is normally considered to be the reference sample.

offset for the phase-shifter, and can also show some time variation due to fluctuations in ambient temperature, humidity, etc, so that it needs to be measured and subtracted periodically. Accordingly, at each angle δ in our phase-shifter scans, generally spanning nearly 8π (*i.e.* 4 periods) in ϕ, the counts of the O and H detectors were measured with both samples raised above the interferometer (samples OUT), and with both samples precisely lowered into place (samples IN). Two sinusoidal curves are thereby generated for each detector and show a sample-induced relative phase difference of

$$\begin{aligned} \Delta\phi &= \Delta\phi_{\mathrm{IN}} - \Delta\phi_{\mathrm{OUT}} \\ &= (\phi_{1,\mathrm{IN}} - \phi_{2,\mathrm{IN}}) - (\phi_{1,\mathrm{OUT}} - \phi_{2,\mathrm{OUT}}) \\ &= (\phi_{1,\mathrm{IN}} - \phi_{1,\mathrm{OUT}}) - (\phi_{2,\mathrm{IN}} - \phi_{2,\mathrm{OUT}}) \\ &= \phi_1 - \phi_2 \end{aligned} \tag{2.5}$$

which via equation (2.4) allows $\Delta\overline{b}$ to be determined. In practice, as discussed in section 2.3, account must also be made of the phase shifts induced by the sample containers, of small systematic differences between beams 1 and 2, and of a possible difference in thickness D_{extra} between the two samples. These experimental considerations will lead to modifications of equations (2.4) and (2.5).

2.3. Experimental details for the $b_{\mathrm{coh,17O}}$ and $b_{\mathrm{coh,18O}}$ measurements

Our bound coherent neutron scattering-length measurements for ^{17}O and ^{18}O were made during two experiments, performed about 8 months apart, both using the S18 instrument with the same interferometer crystal and monocrystalline Si phase-shifter, and both making differential-mode measurements of $H_2{}^{17}O$ versus $H_2{}^{\mathrm{nat}}O$ and of $H_2{}^{18}O$ versus $H_2{}^{\mathrm{nat}}O$. Light water samples are not only easier to acquire, but have a lower average scattering-length density than heavy water samples, so that the phase-difference measurements are less sensitive to possible differences in sample thickness. We used heavy water samples only for the calibration of the Hellma cell dimensions (see section 2.5). Table 1 summarizes the relevant experimental information for the two experiments.

Each water sample was contained in a rectangular Hellma cell, made of pure silica and equiped with two Teflon stoppers. The interior width of these cells is 18.5 mm, and the useful interior height is about 30 mm, both dimensions being considerably larger than the neutron beam size. Although the silica surfaces of the Hellma cells are polished to be optically flat, the interior thickness D of the cells is quoted as 1.00(1) mm (Weill 2007). The 1 % uncertainty in D is a limitation in the accuracy of our measured scattering-length difference $\Delta\overline{b}$ and will be discussed in more detail in section 2.5. The two pairs of Hellma cells (one for experiment I and another for experiment II) were at first thoroughly cleaned with acetone under ultrasound, and then rinsed with either acetone (for drying), distilled water or D_2O, as appropriate, between sample changes. Care was taken not to soil or abrade their surfaces.

For both experiments I and II, we distinguished the two Hellma cells used in the

	Experiment I	**Experiment II**
Date:	Sept/Oct 2008	May/June 2009
$H_2{}^{17}O$ isotopic composition:	Lot I1-9092A: 71.0 % ^{17}O, 28.1 % ^{16}O, 0.9 % ^{18}O	Lot 2333: 91.24 % ^{17}O, 8.35 % ^{16}O, 0.41 % ^{18}O
$H_2{}^{18}O$ isotopic composition:	Lot WP-07-02: 98.1 % ^{18}O, 1.4 % ^{16}O, 0.5 % ^{17}O	Lot WP-08-10: 98.1 % ^{18}O, 1.4 % ^{16}O, 0.5 % ^{17}O
$H_2{}^{nat}O$ samples:	18.2 MΩ-cm, TOC $\lesssim$ 10 ppb	18.2 MΩ-cm, TOC $\lesssim$ 10 ppb
T, N for H_2O:	22(1)°C, 0.10006(3) Å^{-3}	27(1)°C, 0.09993(3) Å^{-3}
D_2O samples:	99.85 % D	99.85 % D
T, N for D_2O:	21(1)°C, 0.09970(3) Å^{-3}	27(1)°C, 0.09960(3) Å^{-3}
Hellma cell type:	404 QS, $D = 1.00(1)$ mm	404 QX, $D = 1.00(1)$ mm
$D_{\rm extra}$:	$+2.9(1)$ μm for $H_2{}^{nat}O$	$-0.3(1)$ μm for $H_2{}^{nat}O$
cell spacing:	32.5(5) mm	31.5(5) mm
incident beam:	6 mm (h) x 6 mm (v)	6 mm (h) x 8 mm (v)
wavelength:	1.914(1) Å	1.912(1) Å

Table 1. Information pertinent to the two neutron interferometry experiments that measured $b_{\rm coh,17O}$ and $b_{\rm coh,18O}$. The atomic number densities N for H_2O and D_2O are taken from Lemmon *et al* (2012) for the indicated temperatures T, where $N_{\rm A} = 0.602214179(30) \times 10^{24}$ mol^{-1} is the value of Avogadro's number used for converting from mol/l to atoms/Å^3. The resistivity and TOC (total organic carbon) purity figures for $H_2{}^{nat}O$ are estimates based on the specifications of the Millipore Simplicity model 185 water purification system used. The isotopic composition of the $H_2{}^{nat}O$ samples was taken to be that of Vienna standard mean ocean water (VSMOW) as described by De Laeter *et al* (2003). The $H_2{}^{17}O$ and $H_2{}^{18}O$ samples were from Euriso-Top (Saclay, France), a distributor of Cambridge Isotope Laboratories (Cambridge, MA) that produces isotopic oxygen gas and then uses it to burn $^{nat}H_2$ gas (supplier: Praxair, Inc., USA) in order to obtain $H_2{}^{17}O$ or $H_2{}^{18}O$ for which the estimated chemical purities are both 99.99 %. The D_2O samples were also from Euriso-Top. The lateral spacing between the cell centers was chosen to correspond, within 1 mm, to the separation between the centers of beams 1 and 2. The letters h and v are used to denote the horizontal and vertical dimensions of the incident beam, respectively.

interferometer, one used for $H_2{}^{nat}O$ and the other used for $H_2{}^{x}O$, where "x" stands for "17" or "18". In all cases, enough of each sample was available to fill its Hellma cell almost completely, leaving only a small air bubble at the top of the cell. Visual observation of these air bubbles confirmed that only a minute portion of the samples (estimate $\lesssim 0.1$ %) evaporated across the Teflon stoppers over a 24 hour period.

Both cells were fixed in place using a custom-made Al cell holder that could be

lowered into the interferometer (but without touching the Si crystal) via an x-y-z translation stage which also allowed rotation about a vertical axis. A standard and reproducible procedure was used to align the samples perpendicular to, and centered on, beams 1 and 2 of the interferometer. Each time a pair of Hellma cells was mounted, a laser reflected from their surfaces confirmed their orientation to within about 3 mrad ($\sim 0.2°$), amounting to less than a 0.01 % error in the measured $\Delta\phi$.

The incident beam dimensions were defined by a set of adjustable Cd slits placed about 5 cm upstream of the interferometer crystal. In experiment II, the intensity profiles of beams 1 and 2 were also measured by translating horizontally across their positions a sheet of neutron-absorbing Cd having a 1 mm slit. The theoretical asymmetry of beam 1 (Rauch and Werner 2000, chp 10) was completely smeared out by the convolving effect of the 6 mm wide beam incident on the interferometer, and the intensity profile of each beam was found to be flat within $\sim$ 5 %. The center-to-center separation of beams 1 and 2 was thus measured to be 31.5(5) mm and this value was used for the center-to-center cell spacing in experiment II, whereas the theoretical beam-separation value of 32.5 mm was used for the cell spacing in experiment I. The use of a center-to-center cell spacing equal to the beam separation to within 1 mm assured that essentially the same part of each cell and sample was probed when placed in either beam 1 or beam 2.

The neutron wavelength from the Si(220) monochromator reflection was measured via diffraction from a single-crystal Si sample at both dispersive and non-dispersive angles, resulting in $\lambda = 1.914(1)$ Å for experiment I and $\lambda = 1.912(1)$ Å for experiment II. The $\lambda/2$ contamination was reduced to less than 0.1 % by placing a set of quartz prisms just upstream of the incident beam slits (without prisms the $\lambda/2$ contamination is normally about 7 %).

The counting rate of each detector was of the order of 1 kHz, and the counting time was typically 2×30 s for each IN+OUT step in a phase-shifter scan of approximately 40 steps which provided a range of almost $4 \times 2\pi$ in $\Delta\phi$. An example of data from a typical phase-shifter scan is shown in figure 2, where $\Delta\phi$ can be precisely obtained from fits to the IN versus OUT sinusoidal curves for either the O or the H detector.

Between 20 and 25 phase-shifter scans were generally performed in series as part of a "run" for a given pair of samples (*i.e.* differential mode), in order to increase statistics and to help average out possible systematic variations in $\Delta\phi$. In addition, in order to compensate for any unexpected effects on $\Delta\phi$ that could result from a sample being mounted in one beam as compared to another, we performed for each pair of samples two runs of phase-shifter scans wherein the Hellma cells containing the samples were switched in position between beams 1 and 2 of the interferometer. Configuration A was chosen to indicate $H_2{}^{nat}O$ in beam 1 and $H_2{}^{x}O$ in beam 2 (resulting in $\Delta\phi_A > 0$ for $b_{coh,xO} > b_{coh,natO}$), with configuration B being the other way around. Data from a typical pair of A&B runs, each run lasting about 20 hours, are shown in figure 3. The uncertainty in the mean value $\overline{\Delta\phi}$ is taken from the standard deviation of the points about the mean in order to include any systematic variations in $\Delta\phi$. Even so, the

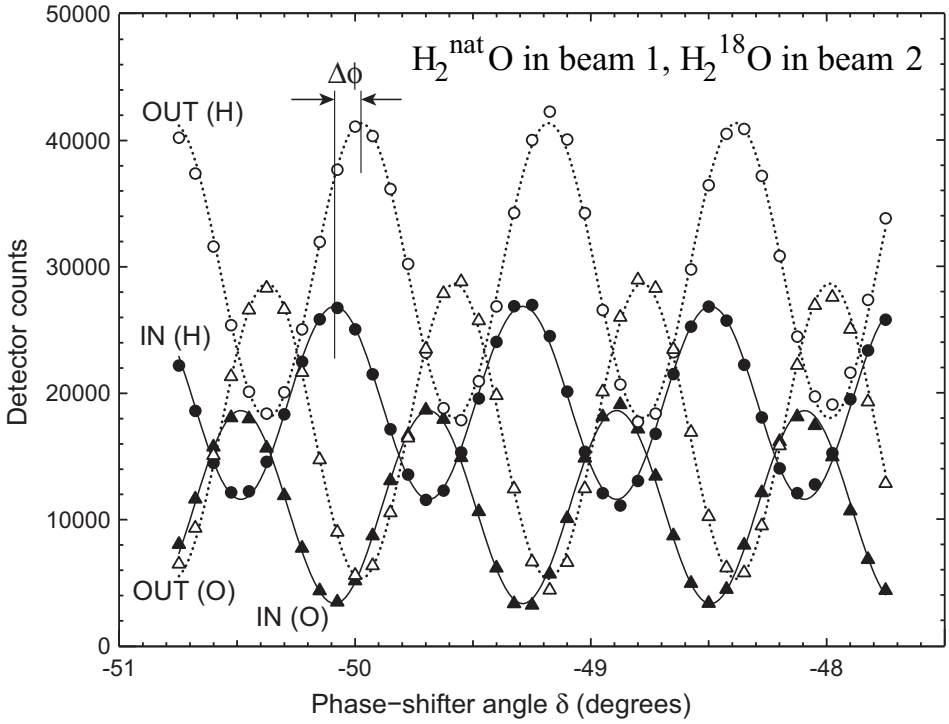

Figure 2. Neutron interferometry data for a typical phase-shifter scan from experiment II for a $H_2{}^{nat}O$ sample in beam 1 and a $H_2{}^{18}O$ sample in beam 2 ("configuration A"). The counts of the O and H detectors are shown as a function of phase-shifter angle for samples lowered IN (solid symbols) and samples raised OUT (open symbols) of the interferometer, and the magnitude of the sample-induced phase difference $\Delta\phi$ is indicated. The error bars due to counting statistics are smaller than the symbol size and are not shown. The phase-shifter scan, lasting about 50 minutes, proceeds from the left to the right along the abscissa, meaning that the IN curves lead in phase ($\Delta\phi = \Delta\phi_{\rm IN} - \Delta\phi_{\rm OUT} > 0$) since they are slightly to the left of the corresponding OUT curves. The smooth curves represent the sinusoidal fits that give $\Delta\phi = +49.60(17)^\circ$, consistent with the $H_2{}^{18}O$ sample having a greater (*i.e.* more positive) scattering-length density than $H_2{}^{nat}O$ (since the measured empty-cell phase difference was of smaller magnitude). Note that the abscissa represents the physical angle δ of the phase-shifter slab in degrees, which has an arbitrary offset angle. The relation between δ and ϕ is not perfectly linear (Rauch and Werner 2000, Eqn. 2.7) and has been duly taken into account in the data analysis. The data of this figure correspond to phase-shifter scan number 10 of the $\Delta\phi_{\rm A}$ curve in figure 3.

resulting uncertainties for $\overline{\Delta\phi}_{\rm A}$ and $\overline{\Delta\phi}_{\rm B}$ shown in figure 3 amount to fractional errors of only slightly more than 1 %. For example, $\overline{\Delta\phi}_{\rm A} = +49.43(59)^\circ$ has a fractional error of 1.2 %.

The silica walls of the Hellma cells, traversed perpendicularly by the neutron beams, were 1.25(1) mm thick. The phase shift ϕ resulting from a total thickness of 2.5(2) mm of silica, as compared to air, can be calculated from equation (2.2) to be about $26.7 \times 2\pi$ for our neutron wavelength. The possible difference in silica thickness between cells makes it necessary to measure and subtract the phase shift of a given Hellma cell from that of the sample contained in this cell. Hence, for each run of phase-shifter scans for a given pair of samples, at least one empty-cell run was performed on the same cells in the same positions in the interferometer, and thus for both the A and B configurations. Note

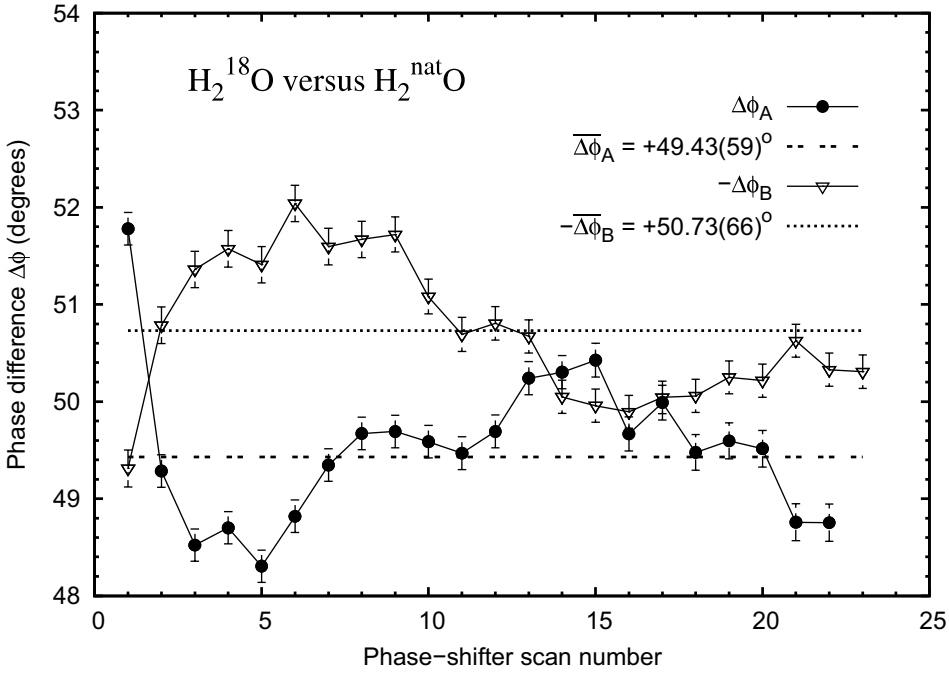

Figure 3. Neutron interferometry data for two "runs" of phase-shifter scans from experiment II for the $H_2{}^{18}O$ sample versus the $H_2{}^{nat}O$ sample. For each phase-shifter scan, the IN and OUT sinusoidal curves for the O detector were least-squares fitted to obtain their phase difference $\Delta\phi$ (as per equation (2.5)) and its uncertainty as indicated by the error bars. The $\Delta\phi_A$ curve corresponds to the $H_2{}^{nat}O$ sample in beam 1 and the $H_2{}^{18}O$ sample in beam 2 ("configuration A") which results in a positive phase difference. Switching the two samples in position between beams 1 and 2 for "configuration B" therefore gives a phase difference $\Delta\phi_B$ that is negative. The mean values $\overline{\Delta\phi}_A = +49.43(59)°$ and $-\overline{\Delta\phi}_B = +50.73(66)°$ agree within their ~ 1 % uncertainties that are taken from the standard deviation of the points about the mean. Note also the overall anti-correlation in the systematic drifts of the $\Delta\phi_A$ and $-\Delta\phi_B$ curves, which suggests the existence of beam-dependent effects (see the text) on the measured phase difference. Phase-shifter scan number 10 of the $\Delta\phi_A$ curve corresponds to the data of figure 2.

that the data shown in figure 3 are before subtraction of the empty-cell contribution to $\Delta\phi$, which was of smaller magnitude than that of the samples.

The interferometer at the S18 instrument, including the suspended vibration-isolated optical table, is housed within a closed concrete room or "bunker" in order to assure relatively stable temperature and humidity conditions. The air temperature within the bunker near the interferometer was measured and continuously recorded at 3 or 4 positions using solid-state thermometers that were calibrated against a single alcohol thermometer of precision ±0.1 °C. In addition for experiment II, water from a temperature-controlled bath was circulated in a support framework surrounding the interferometer crystal. For both experiments, the daily temperature variations inside the bunker near the interferometer were measured to be less than 1 °C, and the overall drifts in measured temperature during the experiments were never more than 4 °C. As shown in table 1, the final estimated uncertainty of ±1 °C in average sample temperature T does not lead to a significant uncertainty in the sample's atomic number density N.

Although the concrete bunker housing the interferometer was quite effective in assuring stable temperature and humidity conditions, intermittant low-frequency sound vibrations (generally non-audible and non-identifiable) are the likely cause of occasional reductions (sometimes by as much as a factor of 2 and lasting hours or even days) in the phase contrast of the interferometer, defined as the amplitude of the O detector's sinusoidal curve (see figure 2) divided by its average value.

2.4. Identifying and treating systematic errors in $\Delta\phi$

Sample changes, and the switching of sample positions between A and B configurations, required a person to enter the bunker and thereby perturb the environment surrounding the interferometer. As a result, the $\Delta\phi$ data point from the first phase-shifter scan of a run was usually anomalous and always discarded from the calculation of the run's mean value. Closer inspection of figure 3 shows the anomalous value of the first point in each of the two $\Delta\phi$ curves, and also an exponential-like dampening of the anomaly over the first 5 or so phase-shifter scans, amounting to a quasi-asymptotic drift in $\Delta\phi$ at the beginning of both runs. We interpret this initial drift, seen in essentially all of our runs, as resulting from an overall re-equilibration of the environment within the bunker following the person's entry and sample manipulation. Moreover, not only the time scale but also the magnitude and sign of this "bunker-equilibration" effect was always the same during experiment II: a drift downwards in $\Delta\phi$ with time of $\sim 3^\circ$ over about 4 hours for both A and B configurations, meaning a drift upwards in $-\Delta\phi_{\mathrm{B}}$ with time as shown in figure 3.

Since $\Delta\phi = \phi_1 - \phi_2$ (by equation (2.5)), a systematic offset in $\Delta\phi$, whether static or varying in time over the course of a run, is *beam-dependent* as it implies a relative shift in phase between beams 1 and 2. Furthermore, since $\Delta\phi = \Delta\phi_{\mathrm{IN}} - \Delta\phi_{\mathrm{OUT}}$ (also by equation (2.5)), this relative shift in phase between beams 1 and 2 must be at least slightly different for samples IN as compared to samples OUT, in order for $\Delta\phi$ to retain a residual beam-dependent effect.

The "bunker-equilibration" effect on $\Delta\phi$ was also present during experiment I and manifested a similar time scale but a greater magnitude ($\sim 5^\circ$) as well as the opposite sign (which could depend on the mounting and alignment details for the interferometer crystal). Note that the interferometer crystal's mounting in experiment II benefitted not only from a temperature-controlled bath but also from being less enclosed and therefore more aerated, both of which could have helped reduce the magnitude of the "bunker-equilibration" effect.

An anti-correlation in systematic offsets or drifts for $\Delta\phi_{\mathrm{A}}$ versus $-\Delta\phi_{\mathrm{B}}$, as a function of phase-shifter scan number, can therefore indicate a potential beam-dependent effect on $\Delta\phi$. Beyond phase-shifter scan 5 in figure 3, the data for $\Delta\phi_{\mathrm{A}}$ show a drift upwards until scan 15 followed by a drift downwards, suggestive of a quasi-sinusoidal variation of amplitude $\sim 2^\circ$ and period ~ 24 hours that appears to be at least partially anti-correlated with the variation in $-\Delta\phi_{\mathrm{B}}$. Since these two runs were started

at roughly the same time on consecutive days, a diurnal effect (*e.g.* temperature) cannot be excluded, but most of the runs during our experiments showed no clear indication of diurnal effects.

There was however an effect from the fluorescent lights mounted on the bunker's ceiling (used simply to illuminate the inside of the bunker): the Al cell holder's IN and OUT positions would shade the interferometer crystal differently, thus heating and distorting the crystal differently between IN and OUT (all within the lapse of the 30 s acquisition time for a point in a phase-shifter scan), and thereby leading to a systematic offset of about 4° in $\Delta\phi = \Delta\phi_{\rm IN} - \Delta\phi_{\rm OUT}$, regardless of any samples or empty Hellma cells being present. Fortunately, this beam-dependent "light effect" was found to be quite reproducible: to within about 0.3° in $\Delta\phi$. The "light effect" was discovered near the beginning of experiment II and then avoided by keeping the lights off during runs, and seems to have been absent, or at least of smaller magnitude, during experiment I.

Tests performed just after experiment II showed that there was also a small beam-dependent effect on $\Delta\phi$ coming from the z motor used to displace the samples vertically above the interferometer crystal. We found that the z motor had a constant holding current even when stationary. This heat source radiated down on the interferometer crystal differently for samples IN as compared to samples OUT, in a similar fashion as for the "light effect", amounting to another systematic offset in $\Delta\phi$ of less than 1° which was however not clearly reproducible.

In summary, we were able to identify two significant and reproducible systematic offsets in $\Delta\phi$ as resulting from the "bunker equilibration" and the "light effect", both having average magnitudes of about 4°. As for other beam-dependent effects on $\Delta\phi$ due to diurnal variations or the z motor, the evidence was less reproducible and/or did not permit a clear identification. Hence, the apparently systematic variations observed in the data of figure 3 after scan 5 can be labelled as "other drifts" in $\Delta\phi$ of unknown origin, showing an amplitude of about 2° and some anti-correlation between $\Delta\phi_{\rm A}$ and $-\Delta\phi_{\rm B}$, a behavior that is typical of that for the majority of A and B runs performed in experiments I and II.

Note that an erroneous increase of 1° in the measured $\Delta\phi = \Delta\phi_{\rm IN} - \Delta\phi_{\rm OUT}$ for these experiments on water samples would lead to an increase of about 0.001 fm in the obtained average scattering-length difference $\Delta\overline{b}$ for the sample in beam 2 as compared to the sample in beam 1, and therefore to an increase of three times as much (0.003 fm) in the scattering-length difference between the oxygen sites of the two water samples. However, since a beam-dependent effect is of opposite sign for $\Delta\phi_{\rm A}$ as compared to $-\Delta\phi_{\rm B}$ as shown by figure 3, it can be suppressed or even cancelled completely by averaging the results of the A and B runs for a given pair of samples. The measured phase difference $\Delta\phi_{\rm x-nat}$ as averaged over A and B configurations for a pair of $H_2{}^{\rm x}O$ versus $H_2{}^{\rm nat}O$ samples, including the subtraction of their corresponding empty cells, is thus:

$$\begin{aligned} \Delta\phi_{\rm x-nat} &= [\ (\overline{\Delta\phi}_{\rm A} - \overline{\Delta\phi}_{\rm A,empty}) - (\overline{\Delta\phi}_{\rm B} - \overline{\Delta\phi}_{\rm B,empty})\ ] \,/\, 2 \\ &= [\ (\overline{\Delta\phi}_{\rm A} - \overline{\Delta\phi}_{\rm B}) - (\overline{\Delta\phi}_{\rm A,empty} - \overline{\Delta\phi}_{\rm B,empty})\ ] \,/\, 2\ , \end{aligned} \tag{2.6}$$

where, for instance, $\Delta\phi_{\rm A} = \Delta\phi_{\rm A,IN} - \Delta\phi_{\rm A,OUT}$ according to equation (2.5), and $\overline{\Delta\phi}_{\rm A}$ is its mean value taken over a run of phase-shifter scans. We can then write for our differential-mode measurements:

$$\Delta\phi_{\rm x-nat} \;=\; \lambda\, N\, \Delta\overline{b}_{\rm x-nat}\, D \tag{2.7}$$

or

$$\Delta\overline{b}_{\rm x-nat} \;=\; \Delta\phi_{\rm x-nat} \,/\, (\,\lambda\, N\, D\,)\;, \tag{2.8}$$

where $\Delta\overline{b}_{\rm x-nat}$ is the difference in average bound coherent scattering length for the $H_2{}^{\rm x}O$ sample as compared to the $H_2{}^{\rm nat}O$ sample, and N is the atomic number density for our light water samples as given by table 1.‡ The fractional uncertainty in $\Delta\overline{b}_{\rm x-nat}$ is limited by the ~ 1 % uncertainty in the measured $\Delta\phi_{\rm x-nat}$ value and by the 1 % uncertainty in D, but equations (2.7) and (2.8) do not take into account properly the difference in interior thickness that likely exists between the two Hellma cells used in the interferometer. Let the interior thicknesses of a given pair of Hellma cells be denoted as D for the cell containing the $H_2{}^{\rm x}O$ sample and $D + D_{\rm extra}$ for the cell containing the $H_2{}^{\rm nat}O$ sample, so that equations (2.7) and (2.8) can be rewritten as

$$\begin{aligned}
\Delta\phi_{\rm x-nat} \;&=\; \phi_{H_2{}^{\rm x}O} \;-\; \phi_{H_2{}^{\rm nat}O} \\
&=\; \lambda\, N \;\; [\, \overline{b}_{H_2{}^{\rm x}O}\, D \;-\; \overline{b}_{H_2{}^{\rm nat}O}\, (D + D_{\rm extra})\,] \\
&=\; \lambda\, N \;\; [\, (\overline{b}_{H_2{}^{\rm x}O} - \overline{b}_{H_2{}^{\rm nat}O})\, D \;-\; \overline{b}_{H_2{}^{\rm nat}O} D_{\rm extra}\,]
\end{aligned} \tag{2.9}$$

and

$$\begin{aligned}
\Delta\overline{b}_{\rm x-nat} \;&=\; \overline{b}_{H_2{}^{\rm x}O} - \overline{b}_{H_2{}^{\rm nat}O} \\
&=\; [\, \Delta\phi_{\rm x-nat} \;+\; \lambda N\, \overline{b}_{H_2{}^{\rm nat}O} D_{\rm extra}\,] \,/\, (\,\lambda\, N\, D\,)\;\;,
\end{aligned} \tag{2.10}$$

where $\Delta\phi_{\rm x-nat}$ is obtained experimentally from equation (2.6), $\phi_{H_2{}^{\rm x}O}$ or $\phi_{H_2{}^{\rm nat}O}$ is the phase shift induced by the $H_2{}^{\rm x}O$ or $H_2{}^{\rm nat}O$ sample of thickness D or $D + D_{\rm extra}$, respectively, and $\overline{b}_{H_2{}^{\rm x}O}$ or $\overline{b}_{H_2{}^{\rm nat}O}$ is the average scattering length of the atoms in the $H_2{}^{\rm x}O$ or $H_2{}^{\rm nat}O$ sample, respectively. Only in the rare case of $D_{\rm extra} = 0$ does equation (2.10) reduce to equation (2.8).

2.5. Calibration of the Hellma cell dimensions

Note that we are considering D and $D_{\rm extra}$ to be the two independent experimental quantities for a pair of Hellma cells, rather than considering their individual interior thicknesses to be independent, as the former is more appropriate for our differential mode of measurement in the interferometer. Equation (2.10) then shows clearly the different

‡ Note that we have ignored any quantum effects (Egelstaff 2002, 2003) that could lead to a difference in atomic number density N between $H_2{}^{17}O$, $H_2{}^{18}O$ and $H_2{}^{\rm nat}O$, since such effects should be considerably smaller than the 0.36 % lower atomic number density difference for D_2O as compared to H_2O (as tabulated by Lemmon *et al* (2012) at a representative temperature of 24.2 °C), and therefore much smaller than the other experimental uncertainties in our experiments. Indeed, the work of Fawdry (2004) suggests that the atomic number density of $H_2{}^{18}O$ is greater than that of $H_2{}^{\rm nat}O$ by only ~ 0.05 %.

effects of an experimental error in the additional interior thickness $D_{\rm extra}$ between cells as compared to an experimental error in the nominal value D common to both cells. The 1 % manufacturer's uncertainty in $D = 1.00(1)$ mm implies a likely value for $D_{\rm extra}$ on the order of ± 10 μm for a given pair of cells. According to the last line of equation (2.10), a neutron of wavelength 1.9 Å traversing an $H_2{}^{\rm nat}O$ sample of additional thickness $D_{\rm extra} = 10$ μm would acquire an additional phase difference of $+6.1^\circ$. Taking the data in figure 3 as an example of an $H_2{}^{\rm x}O$ sample versus an $H_2{}^{\rm nat}O$ sample measured in differential mode, an error of 6.1° amounts to a 12 % fractional error in the obtained value for $\overline{\Delta\phi}_{\rm A}$, and therefore in the measured average scattering-length difference for that run, whereas the last line of equation (2.10) shows that a 1 % fractional error in D leads to only a 1 % fractional error in $\Delta\overline{b}_{\rm x-nat}$, since a change in D changes the interior thickness of both Hellma cells in the interferometer. The difference in interior thickness $D_{\rm extra}$ between the two Hellma cells used in each experiment therefore had to be measured accurately and taken into account via equation (2.10).

When both Hellma cells of a given pair are filled with D_2O, neutron interferometry provides an accurate measurement of their $D_{\rm extra}$, since the large average scattering-length density of D_2O makes the measured phase difference $\Delta\phi$ very sensitive to $D_{\rm extra}$. Equation (2.2) shows that the phase shift ϕ induced by 10 μm of D_2O is 69.6° for our neutron wavelength, more than an order of magnitude greater than that produced by an $H_2{}^{\rm nat}O$ sample, using coherent scattering lengths of $b_{\rm coh,H} = -3.7405(9)$ fm and $b_{\rm coh,D} = 6.653(4)$ fm which take into account the isotopic composition of hydrogen in our samples and which use the new world-average scattering-length values for H and D as reported by Schoen *et al* (2003).

We therefore performed "D_2O runs" of phase-shifter scans for experiments I and II using the same A and B configurations as for the runs on light water samples, and taking into account the empty-cell subtraction via equation (2.6), in order to measure the phase difference $\Delta\phi_{\rm D_2O-D_2O}$ for both cells filled with D_2O. Since $\Delta\overline{b}_{\rm D_2O-D_2O} = 0$, the last line of equation (2.10) can be solved for

$$D_{\rm extra} = -\Delta\phi_{\rm D_2O-D_2O} \,/\, (\,\lambda\, N_{\rm D_2O}\, \overline{b}_{\rm D_2O}\,) \quad , \tag{2.11}$$

where $N_{\rm D_2O}$ and $\overline{b}_{\rm D_2O}$ are the atomic number density and average scattering length, respectively, for our D_2O samples. A value of $D_{\rm extra} = +2.9(1)$ μm was obtained for the pair of Hellma cells used in experiment I§ and $D_{\rm extra} = -0.3(1)$ μm for the pair used in experiment II. The 0.1 μm uncertainty in these $D_{\rm extra}$ values leads to a phase shift

§ The two Hellma cells used in experiment I were the same as those of our earlier experiment (Fischer *et al* 2008) that used a center-to-center cell spacing of 36.0(5) mm, as opposed to 32.5(5) mm in experiment I. In the earlier experiment, a UV-VIS spectrophotometer was used to measure the difference in optical absorption between the two cells filled with a standard absorbing solution, resulting in $D_{\rm extra} = +3.2(1)$ μm. During experiment I, we also performed D_2O runs for a 36.0(5) mm cell spacing and obtained $D_{\rm extra} = +3.3(1)$ μm, thus confirming the result from optical absorption within the experimental error. Note that the variation in $D_{\rm extra}$ of about $3.3 - 2.9 = 0.4$ μm (between optically flat surfaces) over a horizontal distance of about $36 - 32.5 = 3.5$ mm suggests the presence of a small horizontal gradient in the interior thickness of at least one cell in a pair, which confirms the importance of matching the cell spacing to the separation of beams 1 and 2 so that the same thickness of sample

uncertainty of only 0.061° for light water samples, amounting to only 0.12 % of the $\overline{\Delta\phi}_{\mathrm{A}}$ value obtained from the run shown in figure 3. Note that the possibility of a phase wrap of 2π in the measured $\Delta\phi$ for the D_2O runs can be excluded, since that would correspond to a D_{extra} value of about 50 μm, which is far outside the manufacturer's tolerances for the Hellma cells and would be easily measurable using a standard micrometer.

The high accuracy of interferometric results for the D_{extra} of a given pair of Hellma cells validates the idea of a *differential mode* of scattering-length measurement via equation (2.10), since the final uncertainty in the obtained average scattering-length difference $\Delta\overline{b}_{\mathrm{x-nat}}$ is no longer limited by an uncertainty in the value of D_{extra}, but by the uncertainties in D and in the measured $\Delta\phi_{\mathrm{x-nat}}$ which are both at the ~ 1 % level.

2.6. Summary of systematic errors and their effects

Table 2 lists the various sources of systematic error (as identified and discussed in sections 2.3, 2.4 and 2.5) that could affect our scattering-length results. Where an error's magnitude cannot be quantified, its quality is described. The value $\delta(\Delta\phi)$ represents an error's effect on the phase difference measured via sinusoidal fits for a single phase-shifter scan over a range of roughly 4 periods in ϕ (see figure 2). For comparison, the *random* error (from counting statistics, phase-shifter stability, etc) for a given value of $\Delta\phi$ obtained from the fits is about 0.2° on average.

Note that our measured $\Delta\phi$ always came from fitting the IN and OUT sinusoidal curves for the O detector only. As expected for a 3-blade (per beam) interferometer setup such as ours, the H detector has a higher average counting rate as shown in figure 2, but the O detector has the greater contrast since it has the same product of transmission and Bragg-reflection coefficients for beams 1 and 2, thus permitting (in the ideal case) completely destructive interference at the analyzer blade (Rauch and Werner 2000, Eqns. 2.1 and 2.3). Note also that because of the perfect anti-correlation between the O detector counts and the H detector counts after normalisation to their sum, a simultaneous fitting of the O and H sinusoidal curves would add no additional information and thus could not reduce the experimental uncertainty in $\Delta\phi$ from a given phase-shifter scan, a fact that we confirmed.

In table 2 the error propagation from $\delta(\Delta\phi)$ for a given phase-shifter scan to $\delta(\Delta\phi_{\mathrm{x-nat}})$ for a given pair of samples is made via equation (2.6) assuming one pair of 20-hour runs in the A and B configurations for both the samples and their empty cells, where we have taken into account the time scale of the effect during a run and to what extent it was avoided during the experiment. For example, the "light effect" would cancel out when averaging over A and B runs to within its reproducibility of about 0.3°

in each cell is probed for both the A and B configurations. Otherwise, although the effect of any possible gradients in silica wall thickness on the measured $\Delta\overline{b}_{\mathrm{x-nat}}$ would cancel after subtraction of the empty-cell runs, the effect of a gradient in D_{extra} would not cancel and would generally lead to a small but perhaps non-negligible systematic error. Likewise, it is also important that the intensities of beams 1 and 2 do not vary significantly across their respective beam widths, and this was confirmed by scanning a Cd slit horizontally across each beam as described in section 2.3.

Source of error	**Magnitude/quality**	$\delta(\Delta\phi)$	$\delta(\Delta\phi_{\mathrm{x-nat}})$	$\delta(\Delta\overline{b}_{\mathrm{x-nat}})$
"bunker equilibration":	beginning of run	4°	0.2°	0.2 am
"light effect":	controllable	4°	0.3°	0.3 am
other $\Delta\phi$ drifts:	intermittant	2°	0.5°	0.5 am
cell spacing:	1 mm	0.01°	0.01°	0.01 am
cell orientation:	3 mrad	0.005°	0.005°	0.005 am
sample thickness D:	10 μm	–	–	0.6 am
D_{extra}:	0.1 μm	–	–	0.06 am
number density N:	0.00003 Å^{-3}	–	–	0.02 am
wavelength λ:	0.001 Å	–	–	0.03 am
$\lambda/2$ contamination:	< 0.1 %	$< 0.01°$	$< 0.01°$	< 0.01 am

Table 2. Principle sources of systematic error and estimates of their effects δ on the results of our interferometry experiments (see the text for discussion). Note that 1 am $= 10^{-3}$ fm.

in $\Delta\phi$, being thus the value that carries over to $\delta(\Delta\phi_{\mathrm{x-nat}})$. Otherwise we have not assumed any cancellation of beam-dependent effects when estimating $\delta(\Delta\phi_{\mathrm{x-nat}})$, and where differences existed between experiments I and II, we have given an average value.

The error propagation from $\delta(\Delta\phi_{\mathrm{x-nat}})$ to $\delta(\Delta\overline{b}_{\mathrm{x-nat}})$ for a given pair of samples is made using equation (2.10), which is also used to calculate the effects of errors in D_{extra}, λ, N and D. As the latter three parameters each contribute a fractional error to the result, we have calculated their contributions to $\delta(\Delta\overline{b}_{\mathrm{x-nat}})$ using a "worst-case" value of 0.060 fm for $\Delta\overline{b}_{\mathrm{x-nat}}$, corresponding roughly to that for x = 18. The error of 1°C in sample temperature has already been accounted for as a contribution to the error in N.

Note that if the listed errors that contribute to $\delta(\Delta\phi_{\mathrm{x-nat}})$ are considered to be mutually uncorrelated, their total contribution to $\delta(\Delta\overline{b}_{\mathrm{x-nat}})$ becomes 0.62 am or ~ 1 % in the case of x = 18, which is indeed roughly equal to the 0.6 am contribution from the 10 μm error in D alone, once account is made for D_{extra} as discussed in section 2.5. Note also that in the case of an isotopically pure $H_2{}^{\mathrm{x}}O$ sample, the error in the bound coherent scattering-length difference $\Delta b_{\mathrm{coh,xO-natO}} = b_{\mathrm{coh,xO}} - b_{\mathrm{coh,natO}}$ for the $^{\mathrm{x}}O$ isotope is exactly a factor of 3 larger than the corresponding $\delta(\Delta\overline{b}_{\mathrm{x-nat}})$ for the water samples, since exactly 1/3 of the atoms in the samples are oxygen.

It can therefore be ascertained that our values for bound coherent scattering lengths are not "statistically limited" by random error, but have an accuracy that is limited by the systematic errors listed in table 2.

3. Results and discussion

In both experiments I and II, one pair of runs for the A and B configurations were performed for both the $H_2{}^{17}O$ and $H_2{}^{18}O$ samples. Two such pairs of A&B runs were performed for the empty cells in experiment I, as compared to three in experiment II. Upon averaging over A and B configurations and subtraction of the empty-cell contributions as per equation (2.6), the phase differences $\Delta\phi_{\mathrm{x-nat}} = \phi_{\mathrm{H_2{}^xO}} - \phi_{\mathrm{H_2{}^{nat}O}}$ between the $H_2{}^xO$ and $H_2{}^{nat}O$ samples were obtained and are reported in table 3.‖

The values of D_{extra} listed in table 1 for experiments I and II were then used in equation (2.10) to obtain the average scattering-length difference $\Delta\overline{b}_{\mathrm{x-nat}} = \overline{b}_{\mathrm{H_2{}^xO}} - \overline{b}_{\mathrm{H_2{}^{nat}O}}$ between the two samples, from which the bound coherent scattering-length difference $\Delta b_{\mathrm{coh,xO-natO}} = b_{\mathrm{coh,xO}} - b_{\mathrm{coh,natO}}$ for the ^xO isotope can be determined when account is made of the known isotopic composition of the $H_2{}^xO$ sample as given by table 1. Note that since the $H_2{}^{17}O$ samples contained a non-negligible fraction of ^{18}O, and the $H_2{}^{18}O$ samples likewise contained some ^{17}O, a simple iterative procedure was needed to determine simultaneously the $b_{\mathrm{coh,17O}}$ and $b_{\mathrm{coh,18O}}$ scattering lengths that were consistent with the measured results for $\Delta\phi_{\mathrm{17-nat}}$ and $\Delta\phi_{\mathrm{18-nat}}$. This procedure was performed independently for experiments I and II to obtain the $b_{\mathrm{coh,xO}}$ results of table 3.

A few comments are worth making about the values for the experimental uncertainties as shown in table 3. Firstly, the uncertainty in the measured bound coherent scattering-length difference $\Delta b_{\mathrm{coh,xO-natO}}$ is smaller than the uncertainty in the resulting $b_{\mathrm{coh,xO}}$, since the former is obtained directly from a differential measurement between two water samples, and the latter is then calculated from the former using the standard value of $b_{\mathrm{coh,natO}} = 5.805(4)$ fm (Rauch and Waschkowski 2003) that contributes an additional experimental uncertainty.

Note also that the experimental uncertainty of $\pm 1^\circ$ in our measured $\Delta\phi_{\mathrm{x-nat}}$ for experiment I is larger than the $\pm 0.5^\circ$ for experiment II. This is partly due to the phase contrast of the interferometer (*i.e.* that of the O detector's sinusoidal curves) having been a bit worse during experiment I ($\sim$ 50 % as compared to nearly 70 % during experiment II), which is tantamount to lower counting statistics, and experiment I had as well a smaller incident beam height (6 mm as compared to 8 mm). More importantly, note that the uncertainty in the mean $\Delta\phi$ for a given run (*e.g.* $\overline{\Delta\phi}_{\mathrm{A}}$ for the A configuration) of phase-shifter scans is taken from the standard deviation about this mean value, in order to account for the uncertainty due to systematic drifts in $\Delta\phi$, as shown in figure 3. During experiment I, the beam-dependent "bunker-equilibration" effect led to initial drifts in $\Delta\phi$ (see section 2.4) that were of greater magnitude than for experiment II. Also for experiment I, a smaller average number of phase-shifter scans were performed per run for the $H_2{}^xO$ samples and for the empty Hellma cells, as

‖ In order to eliminate the possibility of a phase wrap of 2π in the measured phase difference $\Delta\phi_{\mathrm{18-nat}} = \phi_{\mathrm{H_2{}^{18}O}} - \phi_{\mathrm{H_2{}^{nat}O}}$, we also performed in experiment I an interferometry run using $H_2{}^{nat}O$ versus the $H_2{}^{18}O$ sample diluted by a factor of two with $H_2{}^{nat}O$, and confirmed that the measured phase difference also decreased by a factor of two.

	Experiment I	Experiment II	Recommended
$\Delta\phi_{17-\mathrm{nat}}$:	18.5(10)°	20.8(5)°	
$\Delta\phi_{18-\mathrm{nat}}$:	74.0(10)°	73.6(5)°	
$\Delta\overline{b}_{17-\mathrm{nat}}$:	0.0152(9) fm	0.0192(6) fm	
$\Delta\overline{b}_{18-\mathrm{nat}}$:	0.0658(13) fm	0.0674(9) fm	
$\Delta b_{\mathrm{coh,17O-natO}}$:	0.062(4) fm	0.062(2) fm	0.062(2) fm
$\Delta b_{\mathrm{coh,18O-natO}}$:	0.201(4) fm	0.206(3) fm	0.204(3) fm
$b_{\mathrm{coh,17O}}$:			5.867(4) fm
$b_{\mathrm{coh,18O}}$:			6.009(5) fm

Table 3. Experimental results for the bound coherent neutron scattering lengths of ^{17}O and ^{18}O obtained from the two interferometry experiments performed 8 months apart and having used two different pairs of Hellma cells. The measured phase differences $\Delta\phi_{\mathrm{x-nat}} = \phi_{\mathrm{H_2{}^xO}} - \phi_{\mathrm{H_2{}^{nat}O}}$ are averaged over A and B runs as per equation (2.6) and thus already include the subtraction of the corresponding empty-cell contributions which were $-4.0(5)°$ for experiment I and $-23.55(25)°$ for experiment II. The D_{extra} of table 1 are then taken into account using equation (2.10) to obtain the average scattering-length difference $\Delta\overline{b}_{\mathrm{x-nat}} = \overline{b}_{\mathrm{H_2{}^xO}} - \overline{b}_{\mathrm{H_2{}^{nat}O}}$ between the $H_2{}^xO$ and $H_2{}^{nat}O$ samples, from which the bound coherent scattering-length difference $\Delta b_{\mathrm{coh,xO-natO}} = b_{\mathrm{coh,xO}} - b_{\mathrm{coh,natO}}$ is derived using the known isotopic composition of the $H_2{}^xO$ sample as given by table 1 as well as the new "world-average" value for $b_{\mathrm{coh,H}} = -3.7405(9)$ fm as reported by Schoen *et al* (2003). The value $b_{\mathrm{coh,natO}} = 5.805(4)$ fm from Rauch and Waschkowski (2003) is then used to obtain $b_{\mathrm{coh,17O}}$ and $b_{\mathrm{coh,18O}}$.

compared to experiment II. As a result, a typical standard deviation about the mean $\overline{\Delta\phi}_{\mathrm{A}}$ or $\overline{\Delta\phi}_{\mathrm{B}}$ during experiment I was about $\pm1.2°$ as compared to only $\pm0.6°$ during experiment II (*e.g.* see figure 3 for experiment II), both these uncertainties being reduced by a factor of about $\sqrt{2}$ when averaged over the A and B runs as per equation (2.6). As the empty cells were always run more times than the samples, the uncertainties in the empty-cell phase differences were somewhat smaller for both experiments: $\pm0.5°$ for experiment I and $\pm0.25°$ for experiment II.

Table 3 lists our final recommended values of $b_{\mathrm{coh,17O}} = 5.867(4)$ fm and $b_{\mathrm{coh,18O}} = 6.009(5)$ fm obtained via neutron interferometry, which differ appreciably from the current standard tabulated values (Rauch and Waschkowski 2003) of 5.6(5) fm and 5.84(7) fm, respectively, based largely on Christiansen filter measurements by Koester *et al* (1979). By contrast, there is rather remarkable agreement between our b_{coh} results and those obtained from Bragg diffraction on isotopically enriched UO_2 single crystals by Valentine (1968) for ^{17}O (5.78(15) fm) and O'Connor (1967) for ^{18}O (6.01(13) fm), although their experimental uncertainties are somewhat greater than ours. Such agreement should encourage future use of Bragg diffraction for the measurement of

bound coherent neutron scattering lengths when samples are not well adapted to interferometry measurements.

4. Summary and conclusions

Motivated by the need for accurate values of bound coherent neutron scattering lengths for the oxygen isotopes, especially as regards to the study of the structure of materials using neutron diffraction with isotope substitution (NDIS), we undertook neutron interferometry experiments involving ^{17}O- and ^{18}O-substituted water samples. Having paid particular attention to the data analysis and to the control of possible experimental errors, we propose our results of $b_{\mathrm{coh,17O}} = 5.867(4)$ fm and $b_{\mathrm{coh,18O}} = 6.009(5)$ fm as new standard values for the bound coherent neutron scattering lengths of these oxygen isotopes.

In terms of scattering-length contrast with respect to the accurately-known accepted value of $b_{\mathrm{coh,natO}} = 5.805(4)$ fm, our interferometry results give $\Delta b_{\mathrm{coh,17O-natO}} = 0.062(2)$ fm and $\Delta b_{\mathrm{coh,18O-natO}} = 0.204(3)$ fm, as compared to the respective values of $-0.21(50)$ fm and $0.035(70)$ fm as deduced from the recommended tables (Rauch and Waschkowski 2003). Most promising is our result for the scattering-length contrast between ^{18}O and $^{\mathrm{nat}}$O that is nearly a factor of 6 *greater* than the hitherto tabulated value. This result renders feasible neutron diffraction experiments using ^{18}O isotope substitution and thereby opens up a whole new field of possible structural studies on materials as diverse as water, organic solvents, oxide glasses, organic acids, etc, where the coordination environment of the O atom has an important bearing on the material properties. We have in fact already performed ^{18}O NDIS experiments on light and heavy water (Zeidler *et al* 2011) using the D4c neutron diffractometer (Fischer *et al* 2002) at the Institut Laue-Langevin (Grenoble, France), where use of this method allows for a considerable reduction in the inelastic scattering effects associated with neutron diffraction experiments on water. A detailed account of these diffraction experiments is given by Zeidler *et al* (2012).

Acknowledgments

We appreciate useful discussions with Adrian Barnes (Bristol, UK), as well as the help of Katherine Belisle and Gaetan Seeburn (including their colleagues at Cambridge Isotope Laboratories and at Euriso-Top) as concerns the production and characterisation of the $H_2{}^{17}O$ and $H_2{}^{18}O$ samples.

The Spallation Neutron Source (SNS) is managed by UT-Battelle, LLC, for the U.S. Department of Energy. Contributions of JMS to this research were conducted at the Center for Nanophase Materials Sciences, which is sponsored at Oak Ridge National Laboratory by the Division of Scientific User Facilities, U.S. Department of Energy.

References

Aleksejevs A, Barkanova S, Tambergs J, Krasta T, Waschkowski W and Knopf K 1998 *Z. Naturforschung A* **53** 855–862

De Laeter J R, Böhlke J K, De Bièvre P, Hidaka H, Peiser H S, Rosman K J R and Taylor P D P 2003, *Pure Appl. Chem.* **75** 683–800, and 2009 *Pure Appl. Chem.* **81** 1535–1536

Egelstaff P A 2003 *Phys. Chem. Liquids* **41** 109–121

Egelstaff P A 2002 *Phys. Chem. Liquids* **40** 203–219

Fawdry R M 2004 *Applied Radiation and Isotopes* **60** 23–26

Fischer H E, Neuefeind J, Simonson J M, Loidl R and Rauch H 2008 *J. Phys.: Condens. Matter* **20** 045221

Fischer H E, Barnes A C and Salmon P S 2006 *Rep. Prog. Phys.* **69** 233–299

Fischer H E, Cuello G J, Palleau P, Feltin D, Barnes A C, Badyal Y S and Simonson J M 2002 *Appl. Phys. A.* **74** S160–S162

Koester L, Rauch H and Seymann E 1991 *At. Data Nucl. Data Tabl.* **49** 65–120

Koester L, Knopf K and Waschkowski W 1979 *Z. Physik A* **292** 95–103

Kroupa G, Bruckner G, Bolik O, Zawisky M, Hainbuchner M, Badurek G, Buchelt R J, Schricker A and Rauch H 2000 *Nucl. Instr. and Methods in Phys. Res. A* **440** 604–608

Lemmel H and Wagh A G 2010 *Phys. Rev. A* **82** 033626

Lemmon E W, McLinden M O and Friend D G 2012 *NIST Chemistry WebBook, NIST Standard Reference Database Number 69* ed Linstrom P J and Mallard W G (National Institute of Standards and Technology, Gaithersburg), `http://webbook.nist.gov/chemistry/fluid/` (retrieved June 29, 2012)

Mughabghab S F, Divadeenam M and Holden N E (eds) 1981 *Neutron cross sections, vol. 1, part A* (Academic Press: New York, London)

Neilson G W and Adya A K 1996 *Annual Reports Section C: Royal Society of Chemistry* **93** 101–145

Neuefeind J, Fischer H E, Simonson J M, Idrissi A, Schöps A and Honkimäki V 2009 *J. Chem. Phys.* **130** 174503

O'Connor B H 1967 *Acta Cryst.* **22** 927–928

Rauch H and Waschkowski W 2003 *Neutron data booklet (2nd edition)* ed Dianoux A-J and Lander G (Old City Publishing Group, Philadelphia) chp 1.1, with the on-line version available at `http://www.ati.ac.at/~neutropt/scattering/`

Rauch H and Werner S A 2000 *Neutron interferometry: Lessons in experimental quantum mechanics* (Clarendon Press: Oxford)

Salmon P S, Petri I, de Jong P H K, Verkerk P, Fischer H E and Howells W S 2004 *J. Phys.: Condens. Matter* **16** 195–222

Schoen K, Jacobson D L, Arif M, Huffman P R, Black T C, Snow W M, Lamoreaux S K, Kaiser H and Werner S A 2003 *Phys. Rev. C* **67** 044005

Sears V F 1992 *Neutron News* **Vol 3** (Number 3) 26–37, with the on-line version available at `http://www.ncnr.nist.gov/resources/n-lengths/`

Soper A K 1997 *J. Phys.: Condens. Matter* **9** 2717-2730

Valentine T M 1968 *Harwell Report AERE-R–5770* UK Atomic Energy Research Establishment (Harwell) (5 pages)

Weill B 2007 private communication (Hellma-France)

Zeidler A, Salmon P S, Fischer H E, Neuefeind J C, Simonson J M and Markland T E 2012 *J. Phys.: Condens. Matter* **24** 284126

Zeidler A, Salmon P S, Fischer H E, Neuefeind J C, Simonson J M, Lemmel H, Rauch H and Markland T E 2011 *Phys. Rev. Lett.* **107** 145501, and 2012 *Phys. Rev. Lett.* **108** 259604